

THE DEVELOPMENT OF A CHILL MOULD FOR TOOL STEELS USING NUMERICAL MODELLING

RAZVOJ KOKILE ZA ORODNA JEKLA Z UPORABO NUMERIČNEGA MODELIRANJA

Martin Balcar, Rudolf Železný, Libor Sochor, Pavel Fila, Ludvík Martínek

ŽĎAS, a.s., Strojirenska 6, CZ 59171 Zdar nad Sazavou, Czech Republic
martin.balcar@zdas.cz

Prejem rokopisa – received: 2006-10-11; sprejem za objavo – accepted for publication: 2008-03-25

A long lifetime and tools with optimum quality affect the primary production field and require improvements to the technological conditions of tool-steel ingot production. In the design of a newly developed chill-mould shape the specific casting and crystallization conditions of tool steel, large forging ingots are exploited. The casting and solidification processes were modeled numerically by applying the MAGMA software and the ingot shape was optimized with respect to the real solidification conditions, suppressing the ingot's internal discontinuities and obtaining an acceptable level of structural and chemical homogeneity.

Key words: tool steel, mould, ingot casting, numerical modeling

Dolga trajnostna doba in optimalna kakovost vplivata na primarno proizvodnjo jekla in zahtevata izboljšanja v tehnologiji izdelave jeklenih ingotov. Pri razvoju nove kokile so bili upoštevani pogoji ulivanja in kristalizacije velikih ingotov iz orodnega jekla za izkovke. Procesa ulivanja in strjevanja sta bila modelirana z MAGMA-programom. Oblika ingota pa je bila optimizirana z upoštevanjem realnih razmer pri strjevanju, preprečen je bil nastanek notranjih diskontinuitet in dosežen sprejemljiv nivo strukturne in kemične homogenosti.

Ključne besede: orodno jeklo, kokila, ulivanje ingotov, numerično modeliranje

1 INTRODUCTION

In the frame of the traditional production of equipment and tools for heavy engineering and metallurgy, large forgings of tool steel are also manufactured at ŽĎAS. The tool-steel forgings with good forming properties and tougher requirements in terms of the product's internal quality can only be forged from ingots with a high internal quality. In earlier papers we have discussed the possible causes for the occurrence of inherent defects in heavy ingots of W. Nr. 1.2343 (X37CrMoV5-1) and W. Nr. 1.2344 (X40CrMoV5-1) tool steels according to EN ISO 4957 and in roll forgings of 8CrMoV or 8Cr3MoSiV steels.^{1,2}

The optimization of the ingot-solidification process in the casting mould, the change of the mould shape and avoiding the formation of the defects in the ingot were achieved using the MAGMA software for the simulation of the casting and solidification process of the 8K8.4 forged ingot with a mass of 7.6 t. The project's success was achieved with the design and the verification of a new shape for the 8K9.2 chill mould for the casting of tool-steel ingots with a mass of 8.9 t.

2 DEFECTS IN TOOL STEEL INGOTS

In ZDAS heavy semi-products for tools are produced from ingots of the 8K series, with weights from 1000 kg to 11700 kg, forged on the CKV 630, CKV 1250 and

CKV 1800 presses from the traditional steel grades EN ISO 4957 W. Nr. 1.2842 (90MnCrV8), W. Nr. 1.2842 (X210Cr12), W. Nr. 1.2343 (X37CrMoV51), W. Nr. 1.2344 (X40CrMoV51), W. Nr. 1.2714 (55NiCrMoV7) and special steels for rolls of 8CrMoV, 8CrMoSiV, 8Cr3MoSiV. The increased difficulty of making heavy forgings of tool steels is connected with the specific properties of high-carbon steels, alloyed with chromium, molybdenum and vanadium. Only by ensuring a sufficient forging-reduction ratio of the as-solidified steel, which may have a large number of defects in the final solidification areas in the axial part of the ingot, can a high internal quality of the forging be achieved. To achieve a high reduction ratio it is necessary to ensure a high forming rate and considerable deformation levels per compression.

Tool-steel forming with the CKV 1800 press is limited by the ingot reduction that can be achieved with the pressing force. For this reason, the deformation rate depends strongly on the temperature. A poor forging process may lead, in the case of the bar forgings of tool steels with a large diameter (>200 mm), to a low degree of deformation in the axial part of the forging. With respect to the requirements for the tool's service life and the resistance to considerable dynamic stressing, it is necessary to attain a high internal homogeneity without critical defects. The internal quality of the forgings is checked for crack and cavity occurrence by using ultrasonic examination.



Figure 1: Cross-section at half ingot body height. Image of liquid penetrant test and detail of the axial part of the 8CrMoSiV steel ingot
Slika 1: Prečni prerez pri polovici višine ingota. Posnetek preiskave s tekočim penetrantom in detajl aksialnega dela ingota iz jekla 8CrMoSiV

The analysis of the tool-steel ingot and the forging carried out in connection with the extensive and repeated occurrence of axial defects in forgings has led to interesting findings for the 8K8.4 ingot's solidification, crystallization and forming. In spite of the exploitation of the limited possibilities of material deformation on the CKV 1800 press, the metallographic examinations of the forgings have not shown an insufficient forging reduction in the ingot axis, while ingot examinations have pointed out the causes of the defect occurrence at the forging axis.

Figure 1 shows an image of an 8K8.4 ingot of 8CrMoSiV steel in cross-section at 1/2 ingot body height after a liquid penetrant test, with the considerable occurrence of regular cavities and shrinkage porosity at the ingot axis. The defects are confirmed to the ingot's vertical section, **Figure 2**, with imaging of the distribu-

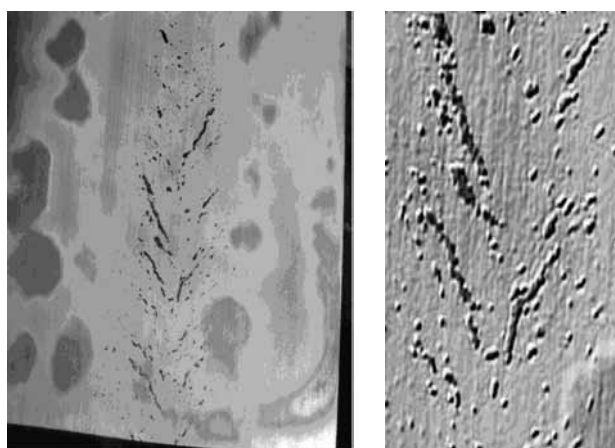


Figure 2: Longitudinal section of the part below the ingot head. Image of the liquid penetrant test and detail of the axial part of the 8CrMoSiV steel ingot

Slika 2: Vzdolžni prerez pod glavo ingota. Posnetek preiskave s tekočim penetrantom in detajl aksialnega dela ingota iz jekla 8CrMoSiV

tion and the shape of the defects throughout the vertical section of the ingot's upper part below the ingot's head.

3 NUMERICAL SIMULATION OF 8K8.4 INGOT CASTING AND SOLIDIFICATION

The conditions for simulations of the existing shape and the design of the optimized shape of the steel chill mould were selected on the basis of practical results and experience of forging the 8K8.4 ingot of 8CrMoSiV tool steel. From the MAGMA database, the GS80CrMo steel was selected because it is very similar to the steel grade investigated in terms of its chemical composition, which is shown for both steels in **Table 1**.

The solidification data were verified on a model of the current polygonal ingot type 8K8.4 of weight 7600 kg. The results of the numerical simulation were obtained as a set of graphical outputs from the MAGMA database and examined in compliance with the practical findings of the ingot's internal quality assessment. On the basis of the analysis, the following parameters for the simulation of the steel ingot's casting and solidification (marking according to the MAGMA database) were determined and selected for further work:

SOLTIME	[s]
LIQTOSOL	[s]
NIYAMA	[1]
PRINCIPAL STRES	[MPa]

Table 1: Chemical composition in mass fractions (w/%) of the 8CrMoSiV steel and the GS80CrMo steel for the simulation from the MAGMA database

Tabela 1: Kemična sestava jekla 8CrMoSiV in jekla GS80CrMo iz baze podatkov MAGMA, ki je bila uporabljena pri simulaciji

	C	Mn	Si	P	S	Cr	Ni	Mo	V
8CrMoSiV	0.78 - 0.85	0.30 - 0.40	0.60 - 0.80	< 0.010	< 0.005	1.80 - 2.10	< 0.30	0.50 - 0.60	0.10 - 0.20
80CrMo	0.80	0.40	0.45	-	-	2.00	-	0.30	-

MISES [MPa]
 $w(C)$ segregation [%]

Figure 3 shows a graphical representation of the numerical simulation results of the 8K8.4 ingot of the GS80CrMo (8CrMoSiV) steel grade. The SOLTIME parameter in the figure shows the evolution of the solidus temperature zone and of the ingot solidification with its dependence on time.

The melt holding time at the liquidus and solidus temperatures interphase dividing line, LIQTOSOL in **Figure 4**, indicates that the metal in the ingot body axis remains at the liquidus–solidus interphase dividing line for a longer time than at the part below the ingot head.

The criterion for micro-shrinkage occurrence – NIYAMA – is shown in **Figure 5**. The vertical axial section through the ingot body in the Niyama criterion representation in scale (0–1) shows the risk points for the occurrence of micro-shrinkage. The Niyama criterion, decisive for the occurrence of micro-shrinkage, is defined as $G/\sqrt{T} (K^{1/2} \cdot s^{1/2} \cdot mm^{-1})$ where $G/(K \cdot mm^{-1})$ is the temperature gradient and $T/(K \cdot s^{-1})$ is the cooling rate. The critical value of the Niyama criterion, decisive for micro-shrinkage occurrence in the castings is $0.775 K^{1/2} \cdot s^{1/2} \cdot mm^{-1}$. Accordingly, the area of overvalues for the critical limit of the Niyama criterion reflects the propensity for micro-shrinkage formation³.

In the conditions of the steel ingots, the Niyama criterion determines the appearance of the material cavities and the micro-porosity. It is, however, not possible to determine with more precision the critical Miyama value on the basis of the available results. When representing the Niyama criterion in scale (0–1), a zone with the values G/\sqrt{T} to $0.5 K^{1/2} \cdot s^{1/2} \cdot mm^{-1}$ in the axial

part of the ingot in **Figure 3**, some shrinkage porosity and cavities may form in the area at approximately 30 % of the body height.

The principal stress parameter in **Figure 5** shows the relative local stressing arising from volume changes in the course of a steel ingot’s solidification. In the cross-section at 1/2 the ingot body’s height, the zone of relatively high local stresses in the ingot body middle part is evident. The occurrence of high stressing in the ingot can also be related to the ingot’s ability to provide the fluid phase in different solidification areas.

The MISES parameter in **Figure 6** shows the relative stress that is used to compare the triaxial stress state with the uniaxial stress state (with the rupture test). The stress values can be compared with the yield and the ultimate strength obtained with the tensile test.

The carbon concentration change throughout the ingot cross-section expressed by the concentration zones in **Figure 8**, does not show the significant non-mixing expected from the ingot’s solidification process.

The results of the numerical simulation agree sufficiently well with the assessed internal quality of the experimental ingots and confirmed the conformity of the theoretical calculations and the practical experience. They also point out some possible causes for the occurrence of axial defects in the ingot and the forging of the tool steel.

The result of the simulations and verifications of the real ingot’s internal quality was the starting stage for the design and construction of a new mould shape.

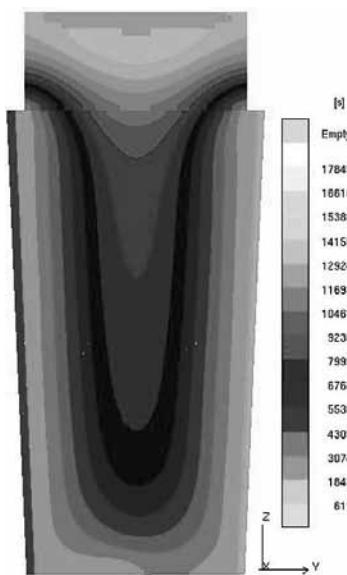


Figure 3: Ingot solidification time 8K8.4 (SOLTIME, s)

Slika 3: Čas strjevanja ingota 8K8.4 (SOLTIME, s)

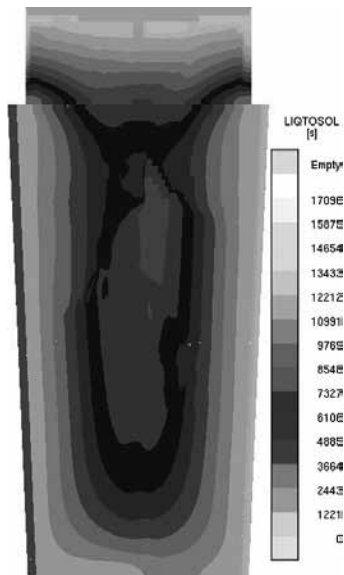


Figure 4: Time $T_{likvidus} - T_{solidus}$ 8K8.4 (LIQTOSOL, s)

Slika 4: Čas $T_{lik} - T_{sol}$ za ingot 8K8.4 (LIQTOSOL, s)

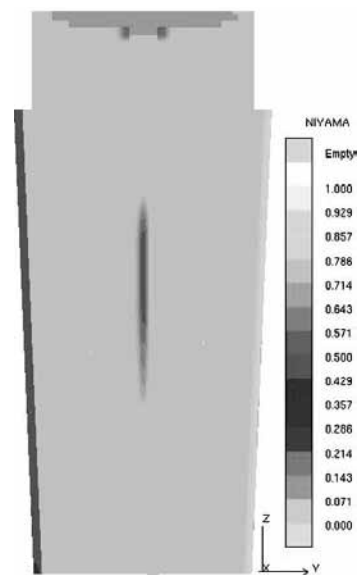


Figure 5: Niyama criterion 8K8.4 (NIYAMA¹)

Slika 5: Niyama–kriterij za ingot 8K8.4 (Niyama¹)

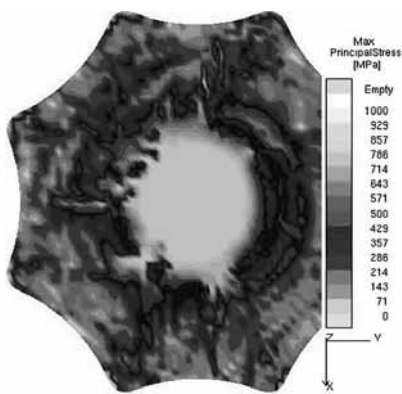


Figure 6: Relative local stress 1/2 ingot height 8K8.4 (PRINCIPAL STRESS, MPa)
Slika 6: Relativna lokalna napetost pri polovici višine ingota 8K8.4 (Glavna napetost, MPa)

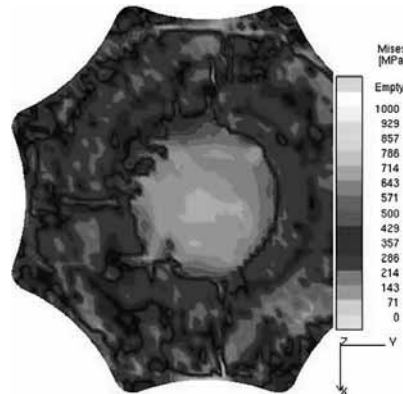


Figure 7: Relative stress 1/2 ingot height 8K8.4 (MISES, MPa)
Slika 7: Relativna napetost pri polovici višine ingota 8K8.4 (Mises, MPa)

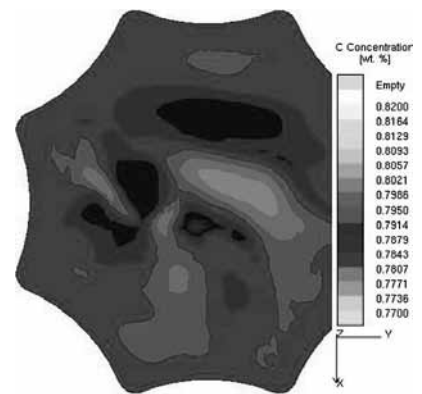


Figure 8: Carbon concentration 1/2 ingot height 8K8.4 ($w(C)/\%$)
Slika 8: Koncentracija ogljika v masnih delcih pri polovici višine ingota 8K8.4 ($w(C)/\%$)

4 DESIGN AND VERIFICATION OF THE INGOT 8K9.2

The design of the new shape of the mould and ingot evolved gradually with the comparison of the results of the calculations for a number of modifications to the mould's geometry. It was based on the present polygonal ingot – type 8K8.4, with a weight of 7600 kg. The main geometrical changes were for the slenderness and the taper of the ingot. The shape was finally modified to be suitable for a simulation of the solidification of the polygonal ingot 8K9.2 of weight of 8850 kg. The comparison between the basic parameters of the ingot 8K8.4 and the new shape design of the ingot 8K9.2 is shown in **Table 2**.

The results of the numerical simulation of casting and solidification of the ingot 8K9.2 of steel GS80CrMo

(8CrMoSiV) evaluated in terms of selected parameters in a similar way as for the original ingot, are shown in **Figures 9 to 14**.

It is clear from **Figure 9** that the change to the mould's geometry has positively changed the shape and course of the curves of the time zones of the solidus temperature. In **Figure 10** the positive effect of the

Table 2: Basic parameters of the ingot 8K8.4 and the design of the ingot 8K9.2

Tabela 2: Osnovni parametri za ingot 8K8.4 in načrt za ingot 8K9.2

Type	Weight and volume				s slenderness	V taper	
	ingot	head		body			
	[kg]	[kg]	[%]	[kg]	[%]	H / D [°]	
8K8.4	7 600	800	11%	6 800	89%	1.9	4.8
8K9.2	8 850	1 200	14%	7 650	86%	1.3	11.0

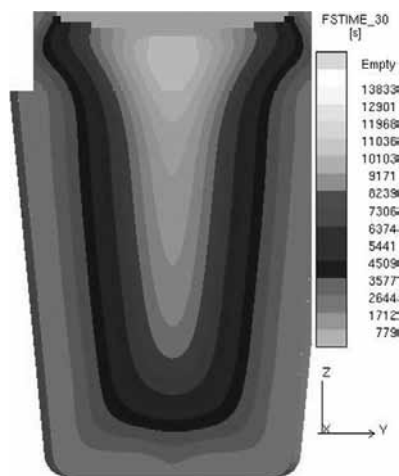


Figure 9: Ingot solidification time 8K9.2 (SOLTIME, s)
Slika 9: Čas strjevanja ingota 8K9.2 (SOLTIME, s)

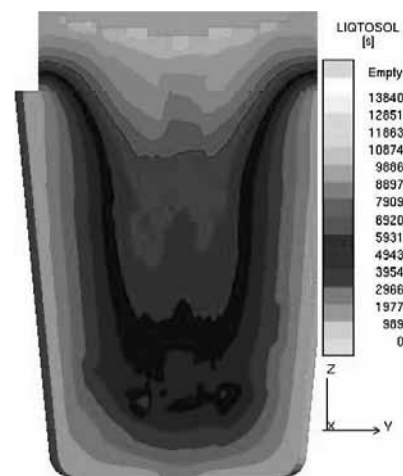


Figure 10: Time $T_{liquidus} - T_{solidus}$ 8K9.2 (LIQTOSOL, s)
Slika 10: Čas $T_{lik.} - T_{sol.}$ za ingot 8K9.2 (LIQTOSOL, s)

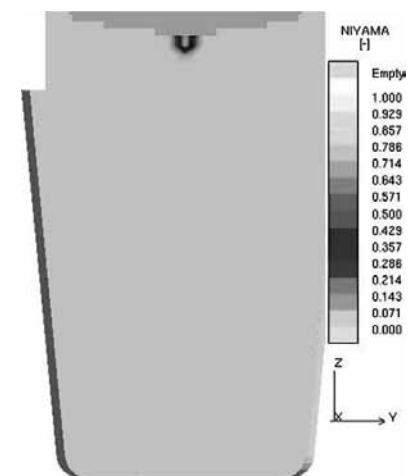


Figure 11: Niyama criterion 8K9.2 (NIYAMA)
Slika 11: Niyama-kriterij za ingot 8K9.2 (Niyama¹)

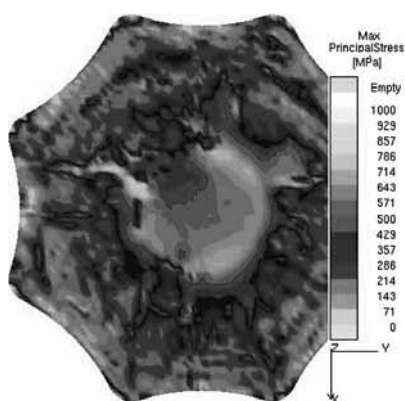


Figure 12: Proportional local stress 1/2 height of the ingot 8K9.2 (PRINCIPAL STRES, MPa)

Slika 12: Relativna lokalna napetost pri polovici višine ingota 8K9.2 (Glavna napetost, MPa)

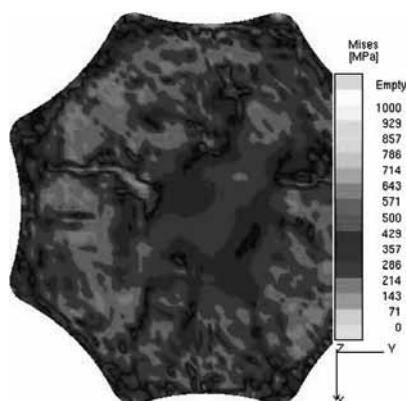


Figure 13: Relative stress 1/2 height of the ingot 8K9.2 (MISES, MPa)

Slika 13: Relativna napetost pri polovici višine ingota 8K9.2 (Mises, MPa)

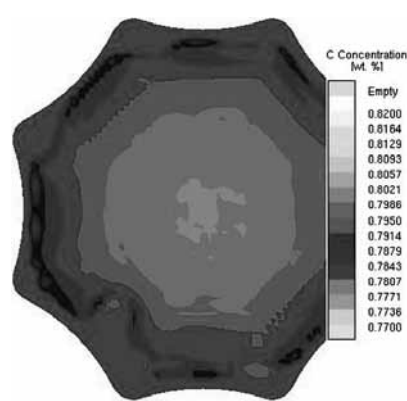


Figure 14: Carbon concentration 1/2 height of the ingot 8K9.2 (w(C)/%)

Slika 14: Koncentracija ogljika v masnih deležih pri polovici višine ingota 8K9.2 (w(C)/%)

enlargement of the ingot taper on the time of the melt persistence the phase-to-phase interface liquidus and solidus is shown. A comparison with **Figures 3 and 4** shows a significant improvement of the feeding of the fluid metal from the head into the body of the ingot. On the basis of the result of the simulation of the casting and the solidification an improvement to the internal quality of the ingot can be expected.

As shown in the ingot section in **Figure 11**, and with a difference compared to the ingot 8K8.4, no axial cavities and shrinkage porosities formed during the solidification of the ingot 8K9.2. In **Figure 12** and **Figure 13** are some interesting changes compared with the original ingot shape. The relative proportional local stress (principal stress) due to volume changes during the solidification of the ingot is reduced considerably. It is assumed that this change is connected with the improved flowability of the fluid metal to the phase-to-phase interface and/or to the point of steel solidification in the ingot. The interrelation between the relative stress and the proportional local stress parameter significantly increases the homogeneity of the stress distribution over the ingot cross-section. Thus, it is logical to expect a lower level of internal stresses in the ingot and an improved homogeneity of the steel's microstructure.

The effect of a change of the mould on the un-mixing and segregation processes is evident from the images in **Figure 14**. The chemical heterogeneity of the ingot 8K9.2 in terms of carbon concentration change over the ingot body cross-section is probably related to the lengthening of the solidification time. This time in the axis and in the middle part of the ingot body, as shown in **Figure 3**, is 9230 s for the ingot 8K8.4 and 11036 s for the ingot 8K9.2, and in **Figure 9** the solidification time for the new ingot shape is increased by 806 s, i.e., by 19.6 % compared to the initial ingot shape.

Based on the achieved improvements in terms of internal quality for the simulated ingot shape, two moulds of shape 8K9.2 were manufactured and their suitability for achieving better internal quality for ingots and forgings of the steel processed in the secondary metallurgy equipment in ŽDAS was tested. The tests were carried out with the steel EN ISO 4957 W. Nr. 1.2344 (X40CrMoV51) and two ingots of 8K9.2 were cast. One ingot was then processed by forming on the CVK 1800 press, using open-die forging technology, to a bar of 350 mm in diameter with the maximum material yield.

Of crucial importance for the evaluation of the effect of the change of the mould shape is the forging's internal quality, which is tested ultrasonically according to the standard SEP 1921. These tests showed that in terms of internal defects the experimental forging from the ingot 8K9.2 of steel EN ISO 4957 W. Nr. 1.2344 (X40CrMoV51) conformed with the levels A/a, B/b, C/c, D/d, E/e. For tool steels, the levels D/d and E/e are acceptable.

Table 3: Ingot utilization – EN ISO 4957 W. Nr. 1.2344 (X40CrMoV5-1) steel forging and internal quality tested ultrasonically per SEP 1921

Tabela 3: Uporaba ingota – EN ISO 4957 W. Nr. 1.2344 (X20CrMoV5-1) jekleni odkovek in podatki o notranji kakovosti, preskušeni z ultrazvokom po SEP 1921

Typ	Hmotnost [kg]	Guaranteed Ultrasonic level	Ingot utilization	
			[kg]	[%]
8K8,4	7600	E/e	0	0
		D/d	4600	61
		C/c	5450	72
		B/b	5950	78
8K9,2	8850	E/e	7300	82

From the verifications carried out and the comparison of results of the statistical data on the earlier production of forgings of steel EN ISO 4957 W. Nr. 1.2344 (X40CrMoV51) shown in Table 3, it is evident that a considerable increase of the ingot yield was achieved after the introduction of the new mould shape.

The bar forging length complied at all levels with the requirements of the ultrasonic test for the ingot volume yield of 82 %. The difference to 100 % could not be used because of the crack extension from the ingot head during the forming process and also for the waste in the ingot foot due to the material flow and the loss during squaring up the face of the forging with machine cutting.

Based on the result of the first assessment it is possible to conclude that an improved internal quality of the ingot 8K9.2 in terms of ultrasonic tests of the internal quality of the tool-steel forging was achieved. This conclusion is confirmed with the results achieved with real shop orders for the tool-steel forgings of heavy bars and blocks with a weight up to 7 t, a bar diameter up to 600 mm and the height of the block up to 500 mm.

5 CONCLUSIONS

The MAGMA software was used for the design of a new shape for the 8K9.2 mould. In spite of the possible modeling errors, it is possible to conclude, based on the results achieved, that a great improvement in the quality

of forgings has been attained as a direct result of the change in the geometry of the forging ingot of type 8K.

The development work will be continued with the aim of a further increase in the quality of the ingots and forgings of selected tool-steel brands and of the verification of the results of a numerical simulation in terms of the internal structure and of the chemical homogeneity related to the solidification and the forming of the ingot.

Acknowledgements

The presented results are part of the TANDEM program of the FT-TA/061 project.

The project was implemented based on state resources with the financial support of the Ministry of Industry and Trade of the Czech Republic.

6 REFERENCES

- ¹ Martínek, L., Balcar, M., Novák, J., Sochor, L.: Rozbor vnitřních nečelistvostí ingotu z nástrojové oceli. 6. Mezinárodní metalurgické sympozium. Rájecké Teplice, 2003
- ² Martínek, L., Balcar, M., Novák, J., Sochor, L.: Vnitřní struktura ingotu z nástrojové oceli. 20. konference Teorie a praxe výroby a zpracování oceli, Rožnov. Tanger, 2003
- ³ Carlson, K.D., Shouzhou Ou, Hardin, R., Beckerman, Ch.: Development of New Feeding – Distance Rules Using Casting Simulation: Part I. Methodology. <http://www.engineering.uiowa.edu/~becker/documents.dir/FeedingPart1.pdf>